Springer

KSME

Journal of Mechanical Science and Technology 32 (8) (2018) 3929~3942
www.springerlink.com/content/1738-494x(Print)/1976-3824(Online)
DOI 10.1007/s12206-018-0744-1

Energy, exergy and exergoeconomic analysis of solar-assisted vertical ground source heat pump system for heating season †

Fatih Ünal[1,*], Galip Temir[2] and Hasan Köten[3]

[1]*Mardin Vocational School, Mardin Artuklu University, Artuklu, Mardin, Turkey*
[2]*Faculty of Engineering, Yıldız Technical University, Beşiktaş, İstanbul, Turkey*
[3]*Faculty of Engineering and Natural Science, İstanbul Medeniyet University, Üsküdar, İstanbul, Turkey*

(Manuscript Received October 5, 2017; Revised March 26, 2018; Accepted April 10, 2018)

Abstract

The purpose of this study is to evaluate the experimental performance of a solar assisted vertical ground source heat pump system (VGSHP) for the winter climatic conditions of Mardin, which is in the South-Eastern Anatolia region of Turkey. For this aim, an experimental analysis was performed on solar assisted VGSHP system, which was designed to meet the heating needs of an experimental room, during the heating season (10.01.2013/03.31.2014). The experimentally obtained results were used to calculate energy, exergy and exergoeconomic analyses of the system and its components. The energy efficiency, exergy efficiency and exergoeconomic factors of the entire system were 67.36 %, 27.40 % and 60.51 %, respectively. In this study, the system was proposed for disseminating the use of alternative technologies supported by renewable energy systems and it has been tested for the first time in Mardin to meet its heating needs with convectional systems. The experimental results showed that the proposed solar assisted VGSHP system can be used for residential heating in Mardin and similar regions. As a result, it has been detected that the system is very effective in both reducing energy consumption and decreasing emissions of green-house gases.

Keywords: Energy; Exergy; Exergoeconomic; Heat pump; Ground source heat pump; Solar assisted ground source heat pump; Thermodynamic analysis

1. Introduction

In parallel with technological developments in the world, global energy consumption is also gradually gaining momentum. Rapid population growth and a correspondingly rapid depletion of traditional energy resources encourage societies to use existing energy potential more effectively, while at the same time forcing them to find new sources of energy. Nowadays due to the gradually decreasing energy resources and increasing energy prices, it has become necessary to use energy more efficiently. An important practise for the correct and economic uses of energy is to reduce energy consumption, in other words, ensuring energy efficiency so as to not hinder the correlated social and economic growth targets [1]. Turkey has a very lucky geographical structure in terms of solar energy, since it receives a significant amount of sunlight. Taking advantage of this energy here is extremely important in terms of its contributions to both environmental pollution and its energy usage affects on the economy. In addition to meeting current energy demands, more work should be done, and more products and services should be obtained with less energy by making productivity improvements. At the same time, the power's environmental damage, which comes from its generation and consumption, must be minimized. For this, alternative technologies, which can be used especially with renewable energy sources should be developed, and it seems necessary to tend to studies which will ensure the use of these systems in industry and everyday life. Most of these energy sources include solar, wind, soil, geothermal, hydrogen, biogas, and sea waves [2, 3].

There are many studies in the relevant literature about GSHPs and also about the energy, exergy and exergoeconomic analyses of different systems. Cervantes and Torres-Reyes [4] experimented with a solar-assisted heat pump system and they studied their experiment's resulting exergy analyses. As a result of these studies, they determined that the irreversibility in the system is mostly in the evaporator of the heat pump. Bi et al. [5] studied solar energy and GSHP systems. In the study, heat fields of the two-dimensional ground heat exchanger were formed and the analyses' results of the system were compared with the experimental results. Also, they estimated the external temperature performance of a solar collector for a GSHP. They have seen that the numerical values of their experimental studies were aligned with the values

*Corresponding author. Tel.: +90 537 381 0623
E-mail address: fatihunal@artuklu.edu.tr, funal81@hotmail.com
† Recommended by Associate Editor Young Soo Chang

for true solar-assisted GSHP. Özgener and Hepbaşlı [6] performed an exergoeconomic analysis of a solar assisted GSHP with a U-curved ground heat exchanger, which had a vertical height of 50 m and a 32 mm nominal diameter, designed for greenhouse heating in Izmir. In their study, they stated that the individual central heating system could not make up for all of the heat loss of the greenhouse at low temperatures but the other assisted HP systems, specifically the solar-assisted ones, were the best solution for the Aegean and Mediterranean regions. Hepbaşlı and Özgener [7] conducted an experimental study on an exergoeconomic analysis of a greenhouse heating system which has a solar assisted GSHP. As a result of their study, they determined that the maximum exergy degradation occurred as a result of electrical, mechanical and entropic effects, and they indicated the amounts of exergy destruction in the components. Özgener et al. [8] conducted exergy and exergoeconomic analyses of the VGSHP system established at the Solar Energy Institute of Ege University in Izmir. As a result of the analysis, they determined the locations of irreversibility in the system. Tsatsaronis [9] defined exergy analysis, exergoeconomic analysis and correlated terminology used in this report. Esen et al. [10] performed energy and exergy analyses of a GSHP in Elazığ. They used the UHE unit at depths of 1 m and 2 m for the GSHP. As a result of these analyses, they found that when the UHE unit was at a depth of 2 m, it caused the GSHP system to have better energy and exergy performances than when it was at a depth of 1 m. Dikici and Akbulut [11] studied the performance characteristics together with the energy and exergy analyses of a solar-assisted HP system in a 60 m^2 test room in Elazığ. As a result of the analyses, they stated that the COP value increases as the loss of exergy in the evaporator decreases. Bi et al. [12] conducted a comparative exergy analysis of a three-phase and full-system GSHP system for buildings' heating and cooling systems. As a result of the study, they found the loss of exergy in its heating mode was greater than the loss of exergy in its cooling mode and that the exergy activity in the whole system was lower than the exergy efficiency of the components. Bakırcı et al. [13] studied the energy analysis of heating applications with a solar-powered vertical type closed-loop GSHP system in Erzurum. In the experimental studies performed, the COP values were found to be 3.0 -3.4 for the heat pump, and 2.7-3.0 for the whole system. As a result, they stated that the system could be used in Erzurum. Kim et al. [14] evaluated the performance evaluation of a dual-compressor VGSHP system at Pusan International University in Korea under real operating conditions. They found the COP values of the HP to be 6.0-10.9 for the cooling season, and the COP values of the complete system to be 4.3-7.4 for the cooling season. In the heating period, they obtained the COP values of the HP at 4.3-8.3 and the COP values of the complete system at 3.0-6.2. Acar and Arslan [15] investigated the performance of the Ranque-Hilsch vortex tube aided drying system by using energy and exergy analyses. Akrami et al. [16] studied energy and exergy evaluation of a tri-generation system driven by the geothermal energy.

In this study, the solar assisted VGSHP was integrated with a fan coil system which has been used in Mardin in order to combine renewable energy systems with alternative Technologies (Mardin is a city that meets its heating and cooling needs with conventional systems). In the experimental study, energy and exergy analyses were performed based on the first and second laws of thermodynamics. Furthermore, a customed exergoeconomic analysis was applied depending on the system's exergy losses and their components. In its economic analyses, the initial investment cost, the cost of exergy losses, and exergoeconomic factors in each unit were calculated. In this study, as opposed to in the relevant literature, the system proposed has been used and tested for the first time in Mardin. It is expected that the system's and analyses' results presented here will be useful and helpful for those who want to benefit from alternative and renewable technologies in our country's South-Eastern Anatolia region and in similar climatic regions.

2. The materials and method

This study analyzed the solar-assisted VGSHP's energy, exergy, and exergoeconomic factors by investigating the results of the experimental studies for the heating season in the province Mardin under the system's real operating conditions. The VGSHP was used to meet the heating needs of the experimental area of 120 m^2. Solar energy assists the VGSHP system during the heating seasons. The system basically consists of four circuits (an underground circuit, heat pump circuit, fan coil circuit and solar energy circuit) with a total of eleven subunits. The general diagram of the system for the heating process is given in Fig. 1. In the underground circuit, heat is drawn from the ground and is transferred to the evaporator ($\dot{Q}_T$) of the heat pump. The heat drawn from the evaporator ($\dot{Q}_L$) gasifies the heat transfer fluid. The temperature and the pressure of the gaseous heat transfer fluid are increased by a compressor and conveyed to the condenser of a fluid heat pump. Here, the heat ($\dot{Q}_H$) generated when condensation takes place is transmitted to the accumulation tank and then to the fan coil circuit ($\dot{Q}_{FC}$). Next, a cooling fluid passes through throttling valves, and the cycle continues. The accumulation tank functions like a balance tank in the system. The heat transferred over the accumulation tank to the fan coil circuit is transmitted to the ground via fan coils ($\dot{Q}_{FC}$). The hot water obtained from the solar energy is transferred to the accumulation tank. The heat pump system is assisted by solar energy in the colder seasons, so solar energy is also used to heat water in the boiler during the warmer seasons.

The test facility (Fig. 2) is a real system which was used to meet the heating needs of the test room in Mardin. The data collection-analysis system was established to collect, organize, and analyze data on a per-second basis from the experimental installation of sensors in the system, including a pressure transmitter (0-40 bar), thermocouple, pvc turbine-type flow

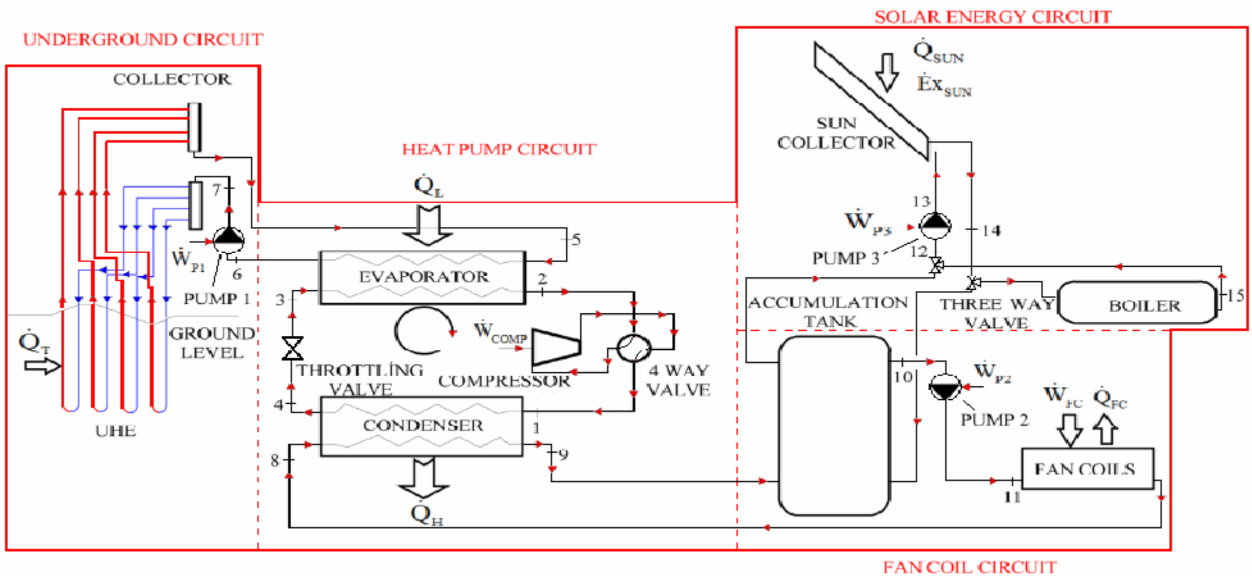

Fig. 1. General system diagram during the heating season.

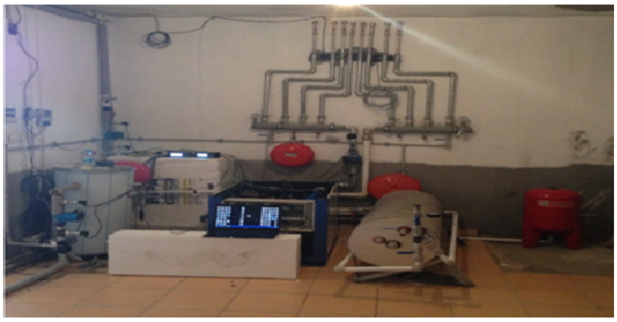

Fig. 2. Test facility.

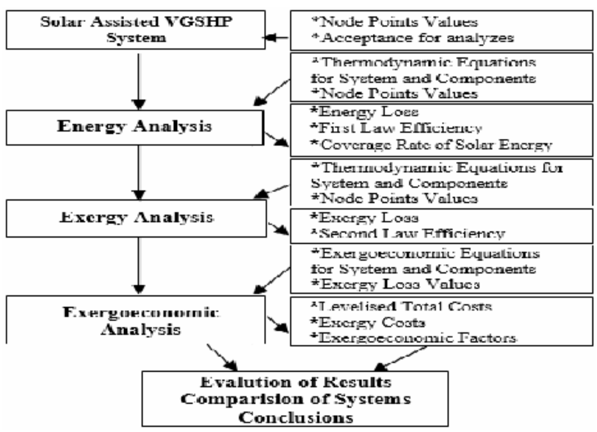

Fig. 3. Flow chart of the analyzes of solar assisted VGSHP.

meter, pyranometer, and dataloggers. In the system, two 16-channel dataloggers were used. Electrical measurements were conducted via a current meter connected to the system. The flow chart of the procedure which was followed for analysis is given in Fig. 3.

2.1 Acceptances in theoretical and experimental studies

Acceptances of this study are given below.

- The Investigated systems are real systems and conform to the continuous open-flow system model. The unmeasured properties of the devices have been taken from catalog values.
- As the underground heat exchanger was completely surrounded by the ground, its heat dissipation was neglected. The pumps worked in a lossy manner. The condenser was isolated and neglected because the amount of loss was very low. The evaporator created a loss of heat, despite being isolated. The compressor was operating with losses. Although the accumulation tank was isolated, there was a loss of heat. There was no enthalpy loss in the throttling valve (h3 = h4).
- The HP system was purchased as a whole. For this reason, the costs of the analyzed parts of the system (compressor, condenser, throttle valve and evaporator) were found by redistributing the ratio of the total cost in pieces to real costs.
- The system's life expectancy is 20 years, its repayment ratio was 6 %, the interest ratio was 3 % and the escalation ratio was 4 %.
- Annual care: The system is to be checked, and the water and cooling fluid are to be replenished if they have decreased. The price of the fluids was $150. During the analysis, the maintenance cost was added on to that of the compressor, which is one of the system's components.
- Two drilling wells with a depth of 100 m each were opened for an underground circuit which costed $20/m. With a_parallel U-tube system, a DN 25 polyethylene composite pipe was used at 200 m vertically and 30 m horizontally, and costed $5/m.
- The cost of each accumulation tank and circulation pump

in the collector line was \$150, and the circulation pump in the ground circuit was \$200.
- The accumulation tank has a capacity of 200 L and is made of stainless steel. The total cost of the accumulation tank, including its connection pipes, insulation, and equipment was \$1000.
- There are 2 fan coils and the total cost of the fan coils, including the piping material, connection equipment, and labor and plaster costs was \$1000.
- Water is used as the heat carrier fluid underground and in the collector and fan coil systems, and R407C is used as refrigerant fluid in the heat pump circuit. Its specific required water temperature is 4.186 kJ / kg. In the exergy analysis, the environmental reference values are T_0 = 0.01 °C and P_0 = 1 bar.

3. Analyses

3.1 Energy analyses of the solar-assisted VGSHP

For the overall analysis of the system, there is no mass input or output in the selected control volume; there is only energy transfer. The first law of thermodynamics is used for an energy analysis. Energy can pass the system boundaries as heat and work. For the first law of thermodynamics, the overall energy conservation for the system can be expressed as follows:

$$\dot{E}_i = \dot{Q}_T + \dot{W}_{p1} + \dot{W}_{comp} + \dot{W}_{p2} + \dot{W}_{p3} + \dot{W}_{FC} + \dot{Q}_{sun} \tag{1}$$

$$\dot{E}_o = \dot{Q}_{FC} + \dot{Q}_{ky} \tag{2}$$

$$\dot{Q}_T + \dot{W}_{p1} + \dot{W}_{comp} + \dot{W}_{p2} + \dot{W}_{p3} + \dot{W}_{FC} + \dot{Q}_{sun} = \dot{Q}_{FC} + \dot{Q}_{ky} . \tag{3}$$

The overall system's first law yield, in other words, the system's efficiency coefficient in the heating process, is calculated as follows:

$$COP_{h,sys} = \frac{\dot{Q}_{fc}}{\dot{W}_{p1} + \dot{W}_{comp} + \dot{W}_{p2} + \dot{W}_{p3} + \dot{W}_{FC}} . \tag{4}$$

In the solar energy system, the useful heat's transference to the collector's heat carrier fluid is depicted here;

$$\dot{Q}_{col} = \dot{m}_{col} \times C_s \times (T_{14} - T_{13}) \tag{5}$$

here as $\dot{m}_{col}$: The fluid flux circulated in the solar circuit, C_s: The specific heat of the heat carrier fluid. The instantaneous yield of the collectors is indicated:

$$\eta_{col} = \frac{\dot{Q}_{col}}{A_{col} \times \overrightarrow{Ht}_{oblique}} \tag{6}$$

here as A_{col} : Collector area, $\overrightarrow{Ht}_{oblique}$: The total amount of energy from solar radiation coming to the oblique collector surface, which can be calculated by the help of conversion factor, is shown [17]:

Table 1. The R conversion factor [18].

Lattude	Season	θ_z °	s			
			15°	30°	45°	60°
36°	June-August	19.12	1.096	1.039	0.952	0.800
	October-March	51.43	1.293	1.496	1.597	1.589
	All year	36.00	1.154	1.229	1.221	1.129
38°	June-August	20.00	1.060	1.059	0.964	0.815
	October-March	51.87	1.296	1.503	1.608	1.603
	All year	38.04	1.168	1.257	1.260	1.177
40°	June-August	22.84	1.075	1.077	1.005	0.865
	October-March	53.44	1.315	1.540	1.661	1.668
	All year	40.00	1.183	1.286	1.301	1.227
42°	June-August	24.28	1.083	1.096	1.026	0.891
	October-March	55.98	1.349	1.607	1.755	1.783
	All year	42.00	1.199	1.316	1.344	1.280

$$\overrightarrow{Ht}_{oblique} = \overrightarrow{Ht}_{horizontal} \times R . \tag{7}$$

In the equation above; $\overrightarrow{Ht}_{Horizontal}$ indicates the total average value of the horizontal plane's solar radiation taken from the meteorology, and R indicates the conversion factor. R was used to convert $\overrightarrow{Ht}_{horizontal}$ to $\overrightarrow{Ht}_{oblique}$ depending on latitude, inclination angle of the flat collector(s) and season. If the R conversion factor is known, the total amount of energy from solar radiation coming to the collector surface at an inclined position can be calculated. The R conversion factor is given in Table 1, and its value changes according to the inclination angle of the flat collector, latitude, and the season.

The Province Mardin is positioned at 37° latitude. In the solar energy system, the collector is positioned at an inclination angle(s) of 45°. It is taken from Table 1 as 1.603 by the interpolation of the heating seasons (October-March). The required coverage ratio of solar energy is found by the following equation:

$$\text{CR= (Energy obtained)/(Required energy)} . \tag{8}$$

3.2 Exergy analysis of the solar-assisted VGSHP

Energy, which is defined as the ability to do work, consists of two parts as energy and exergy. Exergy is the part of energy that can be used [19]. In this study, kinetic, potential and chemical exergies were neglected, and calculations were made with physical exergy. The physical exergy of pure substances is generally briefly formulated as follows:

$$ex^{PH} = (h - h_0) - T_0(s - s_0) \quad (\text{kJ/kg}) . \tag{9}$$

The total physical exergy flow is given as follows:

$$\dot{E}x^{PH} = \dot{m}ex^{PH} . \tag{10}$$

For any system components, the ratio of exergy loss amount is stated as:

$$\dot{E}x_{ky} = \sum(1-\frac{T_0}{T})\dot{Q} - \dot{W} + \sum \dot{m}_i ex_i - \sum \dot{m}_o ex_o \ . \tag{11}$$

Exergy efficiency is expressed by the following formula:

$$\eta_{II} = 1 - \frac{\text{Exergy loss}}{\text{Exergy input}} = \frac{\text{Exergy output}}{\text{Exergy input}} \ . \tag{12}$$

For the analyzed system, exergy loss can be written by using Eq. (11).

$$\dot{E}x_{ky,sys} = \dot{Q}_T(1-\frac{T_0}{T_T}) + \dot{Q}_{sun}(1-\frac{T_0}{T_{sun}}) + \dot{W}_{in} - \dot{Q}_{FC} \times (1-\frac{T_0}{T_{FC}}) \ . \tag{13}$$

By taking into account the yields of pumps and compressor, exergy efficiency is calculated by Eq. (12) as follows:

$$\eta_{II,sys} = \frac{\dot{Q}_{FC}(1-\dfrac{T_0}{T_{FC}})}{\dot{Q}_T(1-\dfrac{T_0}{T_T}) + \dot{W}_{in} + \dot{Q}_{sun}(1-\dfrac{T_0}{T_{sun}})} \ . \tag{14}$$

The overall systems' energy and exergy balances and units are given in Table 2.

3.3 Exergoeconomic analysis of solar assisted VGSHP

In a continuous-flow system, energy can be transferred in the form of material input-output, and of work and heat transfers. Substance and energy transfers in the system occur at the same time as the exergy transfer. While some of the transferred exergy becomes a system output, some of it disappears within the system due to irreversibilities. If the unit exergy price is showed by "c", the total exergy price can be expressed for the component of a system, "k", in the following equation:

$$\dot{C}_k = c_k \cdot \dot{E}x_k = c_k \cdot m_k \cdot ex_k \ . \tag{15}$$

Above $\dot{E}x$ is the exergy flow, and $\dot{C}$ is the price of the exergy flow. In accordance with the above equation, the following expressions can be written:

$$\dot{C}_k = c_k \dot{E}x_k = c_k\left(m_k ex_k\right) \tag{16}$$

$$\dot{C}_w = c_w \cdot \dot{W} \tag{17}$$

$$\dot{C}_q = c_q \cdot \dot{E}x_q \ . \tag{18}$$

When the cost of exergy is calculated, the components in a system are considered separately. The cost equilibrium equation for the "k" system component can be written as follows:

$$\sum C_{e,k} + C_{w,k} = C_{q,k} + \sum C_{i,k} + Z_k \ . \tag{19}$$

Here, the expression Z_k is a levelized monetary value which includes the investment, operation, and maintenance costs of the "k" component. The value "Z" representation of a selected parameter, such as an annual working time, system life expectancy, interest, and escalation.

$$Z = A\left[\frac{\text{Initial investment cost}}{\text{Sys life} \times \text{annual working hour}} + \frac{\text{Electricity+maintenance costs}}{\text{Annual working hour}}\right] \tag{20}$$

In order to calculate the Z value, it is necessary to determine the initial investment and operation costs of the system and of the selected component. The initial system and component investment costs include operating and repair/maintenance costs. When the Z value is calculated, the sum of the initial investment and operating costs in a set unit of time is multiplied by "a levelized value factor (A)". The levelized value factor is expressed in the following equation [20].

$$A = \frac{CELF}{1+r_i} \ . \tag{21}$$

In this equation, "CELF" is the constant escalation levelling factor, and "r_i" is the interest ratio. The CELF is expressed in the following equation:

$$CELF = \frac{k\left(1-k^n\right)}{1-k} CRF \ . \tag{22}$$

In this equation, the "CRF" value contains the capital recovery factor, and the "k" value contains the levelized price correction factor. The "n" value indicates the foreseeable lifetime for the system or component.

The capital recovery factor (CRF) is expressed in the following equation, wherein the "i_{eff}" value indicates the repayment ratio:

$$CRF = \frac{i_{eff}\left(1+i_{eff}\right)^n}{\left(1+i_{eff}\right)^n - 1} \ . \tag{23}$$

The price correction factor is expressed in the following equation [20]:

$$k = \frac{\left(1+r_n\right)}{\left(1+i_{eff}\right)} \ . \tag{24}$$

The cost resources of a component can be divided into two categories. While in the first category there are non-exergent

Table 2. Energy and exergy balances of solar assisted VGSHP.

Unit	Energy and exergy balances
All system 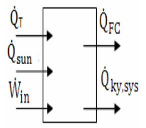	$\dot{Q}_T + \dot{W}_{in} + \dot{Q}_{sun} = \dot{Q}_{FC} + \dot{Q}_{ky,sys}$ $COP_{H,SYS} = \frac{\dot{Q}_{FC}}{\dot{W}_{in}}$ $\dot{E}x_T + \dot{W}_{in} + \dot{E}x_{sun} = \dot{E}x_{FC} + \dot{E}x_{ky,sys}$ $\eta_{II,SYS} = \frac{\dot{E}x_{FC}}{\dot{E}x_T + \dot{W}_{in} + \dot{E}x_{sun}}$
Heat pump circuit 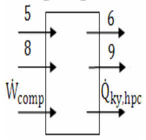	$\dot{E}_5 + \dot{W}_{comp} + \dot{E}_8 = \dot{E}_9 + \dot{E}_6 + \dot{Q}_{ky,hpc}$ $\eta_{H,HPC} = \frac{\dot{E}_9 - \dot{E}_8}{\dot{W}_{comp} + \dot{E}_5 - \dot{E}_6}$ $\dot{E}x_5 + \dot{W}_{comp} + \dot{E}x_8 = \dot{E}x_9 + \dot{E}x_6 + \dot{E}x_{ky,hpc}$ $\eta_{II,H,HPC} = \frac{\dot{E}x_9 + \dot{E}x_6}{\dot{W}_{comp} + \dot{E}x_5 + \dot{E}x_8}$
Compressor 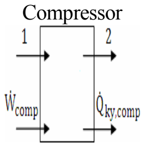	$\dot{E}_2 + \dot{W}_{comp} = \dot{E}_1 + \dot{Q}_{ky,comp}$ $\eta_{H,COMP} = \frac{\dot{E}_1 - \dot{E}_2}{\dot{W}_{comp}}$ $\dot{E}x_2 + \dot{W}_{comp} = \dot{E}x_1 + \dot{E}x_{ky,comp}$ $\eta_{II,H,COMP} = \frac{\dot{E}x_1}{\dot{W}_{comp} + \dot{E}x_2}$
Condenser 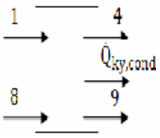	$\dot{E}_1 + \dot{E}_8 = \dot{E}_9 + \dot{E}_4 + \dot{Q}_{ky,cond}$ $\eta_{H,COND} = \frac{\dot{E}_9 - \dot{E}_8}{\dot{E}_1 - \dot{E}_4}$ $\dot{E}x_1 + \dot{E}x_8 = \dot{E}x_9 + \dot{E}x_4 + \dot{E}x_{ky,cond}$ $\eta_{II,H,COND} = \frac{\dot{E}x_9 + \dot{E}x_4}{\dot{E}x_1 + \dot{E}x_8}$
Throttling valve 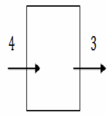	$\dot{E}_4 = \dot{E}_3$ $\eta_{H,TV} = \frac{\dot{E}_3}{\dot{E}_4}$ $\dot{E}x_4 = \dot{E}x_3 + \dot{E}x_{ky,tv}$ $\eta_{II,H,TV} = \frac{\dot{E}x_3}{\dot{E}x_4}$
Evaporator 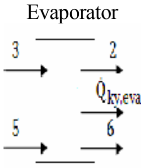	$\dot{E}_3 + \dot{E}_5 = \dot{E}_2 + \dot{E}_6 + \dot{Q}_{ky,eva}$ $\eta_{H,EVA} = \frac{\dot{E}_2 - \dot{E}_3}{\dot{E}_5 - \dot{E}_6}$ $\dot{E}x_3 + \dot{E}x_5 = \dot{E}x_2 + \dot{E}x_6 + \dot{E}x_{ky,eva}$ $\eta_{II,H,EVA} = \frac{\dot{E}x_2 + \dot{E}x_6}{\dot{E}x_3 + \dot{E}x_5}$
Underground circuit 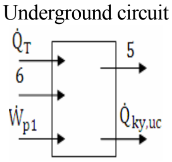	$\dot{Q}_T + \dot{W}_{p1} + \dot{E}_6 = \dot{E}_5 + \dot{Q}_{ky,uc}$ $\eta_{H,UC} = \frac{\dot{E}_5 - \dot{E}_6}{\dot{W}_{p1} + \dot{Q}_T}$ $\dot{E}x_T + \dot{W}_{p1} + \dot{E}x_6 = \dot{E}x_5 + \dot{E}x_{ky,uc}$ $\eta_{II,H,UC} = \frac{\dot{E}x_5}{\dot{E}x_T + \dot{W}_{p1} + \dot{E}x_6}$
Pump 1 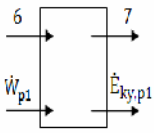	$\dot{E}_6 + \dot{W}_{p1} = \dot{E}_7 + \dot{E}_{ky,p1}$ $\eta_{P1} = \frac{\dot{E}_7 - \dot{E}_6}{\dot{W}_{p1}}$ $\dot{E}x_6 + \dot{W}_{p1} = \dot{E}x_7 + \dot{E}x_{ky,p1}$ $\eta_{II,P1} = \frac{\dot{E}x_7}{\dot{E}x_6 + \dot{W}_{p1}}$
Underground heat exchanger 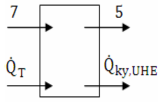	$\dot{Q}_T + \dot{E}_7 = \dot{E}_5 + \dot{Q}_{ky,uhe}$ $\eta_{H,UHE} = \frac{\dot{E}_5 - \dot{E}_7}{\dot{Q}_T}$ $\dot{E}x_T + \dot{E}x_7 = \dot{E}x_5 + \dot{E}x_{ky,uhe}$ $\eta_{II,H,UHE} = \frac{\dot{E}x_5}{\dot{E}x_T + \dot{E}x_7}$
Fan coil circuit 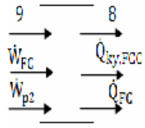	$\dot{E}_9 + \dot{W}_{p2} + \dot{W}_{FC} = \dot{E}_8 + \dot{Q}_{FC} + \dot{Q}_{ky,fcc}$ $\eta_{H,FCC} = \frac{\dot{Q}_{FC}}{\dot{E}_9 - \dot{E}_8 + \dot{W}_{p2} + \dot{W}_{FC}}$ $\dot{E}x_9 + \dot{W}_{p2} + \dot{W}_{FC} = \dot{E}x_8 + \dot{E}x_{FC} + \dot{E}x_{ky,fcc}$ $\eta_{II,H,FCC} = \frac{\dot{E}x_8 + \dot{E}x_{FC}}{\dot{E}x_9 + \dot{W}_{p2} + \dot{W}_{FC}}$
Accumulation tank 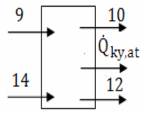	$\dot{E}_9 + \dot{E}_{14} = \dot{E}_{10} + \dot{E}_{12} + \dot{Q}_{ky,at}$ $\eta_{H,AT} = \frac{\dot{E}_{14} - \dot{E}_{12}}{\dot{E}_{10} - \dot{E}_9}$ $\dot{E}x_9 + \dot{E}x_{14} = \dot{E}x_{10} + \dot{E}x_{12} + \dot{E}x_{ky,at}$ $\eta_{II,H,AT} = \frac{\dot{E}x_{10} + \dot{E}x_{12}}{\dot{E}x_9 + \dot{E}x_{14}}$
Pump 2 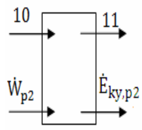	$\dot{E}_{10} + \dot{W}_{p2} = \dot{E}_{11} + \dot{E}_{ky,p2}$ $\eta_{P2} = \frac{\dot{E}_{11} - \dot{E}_{10}}{\dot{W}_{p2}}$ $\dot{E}x_{10} + \dot{W}_{p2} = \dot{E}x_{11} + \dot{E}x_{ky,p2}$ $\eta_{II,P2} = \frac{\dot{E}x_{11}}{\dot{E}x_{10} + \dot{W}_{p2}}$
Fan coils 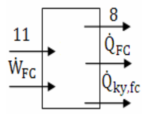	$\dot{E}_{11} + \dot{W}_{FC} = \dot{E}_8 + \dot{Q}_{FC} + \dot{Q}_{ky,fc}$ $\eta_{H,FC} = \frac{\dot{Q}_{FC}}{\dot{E}_{11} - \dot{E}_8 + \dot{W}_{FC}}$ $\dot{E}x_{11} + \dot{W}_{FC} = \dot{E}x_8 + \dot{E}x_{FC} + \dot{E}x_{ky,fc}$ $\eta_{II,H,FC} = \frac{\dot{E}x_8 + \dot{E}x_{FC}}{\dot{E}x_{11} + \dot{W}_{FC}}$
Solar energy circuit 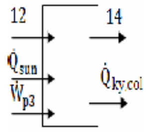	$\dot{E}_{12} + \dot{W}_{p3} + \dot{Q}_{sun} = \dot{E}_{14} + \dot{Q}_{ky,SEC}$ $\eta_{H,SEC} = \frac{\dot{E}_{14} - \dot{E}_{12}}{\dot{W}_{p3} + \dot{Q}_{sun}}$ $\dot{E}x_{12} + \dot{W}_{p3} + \dot{E}x_{sun} = \dot{E}x_{14} + \dot{E}x_{ky,SEC}$ $\eta_{II,H,SEC} = \frac{\dot{E}x_{14}}{\dot{E}x_{12} + \dot{W}_{p3} + \dot{E}x_{sun}}$
Pump 3 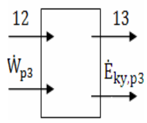	$\dot{E}_{12} + \dot{W}_{p3} = \dot{E}_{13} + \dot{E}_{ky,p3}$ $\eta_{P3} = \frac{\dot{E}_{13} - \dot{E}_{12}}{\dot{W}_{p3}}$ $\dot{E}x_{12} + \dot{W}_{p3} = \dot{E}x_{13} + \dot{E}x_{ky,p3}$ $\eta_{II,P3} = \frac{\dot{E}x_{13}}{\dot{E}x_{12} + \dot{W}_{p3}}$
Solar collectors 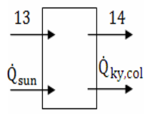	$\dot{E}_{13} + \dot{Q}_{sun} = \dot{E}_{14} + \dot{E}_{ky,col}$ $\eta_{H,COL} = \frac{\dot{E}_{14} - \dot{E}_{13}}{\dot{W}_{p3} + \dot{Q}_{sun}}$ $\dot{E}x_{13} + \dot{E}x_{sun} = \dot{E}x_{14} + \dot{E}x_{ky,col}$ $\eta_{II,H,COL} = \frac{\dot{E}x_{14}}{\dot{E}x_{13} + \dot{E}x_{sun}}$

Table 3. Exergoeconomic balances of solar assisted VGSHP.

Unit	Exergoeconomic balances
All system 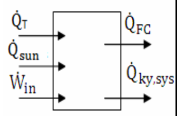	$c_T\dot{E}x_T + c_{w,in}\dot{W}_{in} + c_{sun}\dot{E}x_{sun} + \dot{Z}_{sys} = c_{FC}\dot{E}x_{FC}$ $\dot{C}_{Q,T} + \dot{C}_{w,in} + \dot{Z}_{sys} + \dot{C}_{Q,sun} = \dot{C}_{Q,FC}$ $\dot{C}_{sys} = \left(\dot{c}_{Q,T} + \dot{c}_{w,in}\right)\dot{E}x_{ky,sys}$ $f_{c,SYS} = \dfrac{\dot{Z}_{sys}}{\dot{Z}_{sys} + \dot{C}_{sys}}$
Heat pump circuit 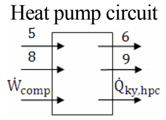	$c_5\dot{E}x_5 + c_{w,comp}\dot{W}_{comp} + c_8\dot{E}x_8 + \dot{Z}_{hpc} = c_6\dot{E}x_6 + c_9\dot{E}x_9$ $(c_8 = c_9; c_5 = c_6)$ $\dot{C}_5 + \dot{C}_{w,comp} + \dot{C}_8 + \dot{Z}_{hpc} = \dot{C}_6 + \dot{C}_9$ $\dot{C}_{hpc} = \left(\dot{c}_5 + \dot{c}_8 + \dot{c}_{w,comp}\right)\dot{E}x_{ky,hpc}$ $f_{c,HPC} = \dfrac{\dot{Z}_{hpc}}{\dot{Z}_{hpc} + \dot{C}_{hpc}}$
Compressor 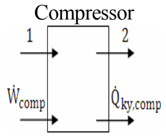	$c_1\dot{E}x_1 + c_{w,comp}\dot{W}_{comp} + \dot{Z}_{comp} = c_2\dot{E}x_2$ $c_1 = c_2; c_{(w,komp)} = 1.944x10^{(-5)}\$/h$ $\dot{C}_1 + \dot{C}_{w,comp} + \dot{Z}_{comp} = \dot{C}_2$ $\dot{C}_{comp} = \left(\dot{c}_1 + \dot{c}_{w,comp}\right)\dot{E}x_{ky,comp}$ $f_{c,COMP} = \dfrac{\dot{Z}_{comp}}{\dot{Z}_{comp} + \dot{C}_{comp}}$
Condenser 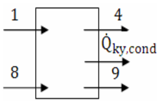	$c_1\dot{E}x_1 + c_8\dot{E}x_8 + \dot{Z}_{cond} = c_4\dot{E}x_4 + c_9\dot{E}x_9$ $c_1 = c_4; c_8 = c_9$ $\dot{C}_1 + \dot{C}_8 + \dot{Z}_{cond} = \dot{C}_4 + \dot{C}_9$ $\dot{C}_{kond} = \left(\dot{c}_1 + \dot{c}_8\right)\dot{E}x_{ky,cond}$ $f_{c,COND} = \dfrac{\dot{Z}_{cond}}{\dot{Z}_{cond} + \dot{C}_{kond}}$
Throttling valve 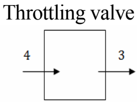	$c_4\dot{E}x_4 + \dot{Z}_{tv} = c_3\dot{E}x_3$ $c_3 = c_4$ $\dot{C}_4 + \dot{Z}_{tv} = \dot{C}_3$ $\dot{C}_{tv} = \dot{c}_4\dot{E}x_{ky,tv}$ $f_{c,TV} = \dfrac{\dot{Z}_{tv}}{\dot{Z}_{tv} + \dot{C}_{tv}}$
Evaporator 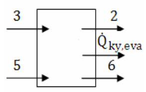	$c_3\dot{E}x_3 + c_5\dot{E}x_5 + \dot{Z}_{eva} = c_2\dot{E}x_2 + c_6\dot{E}x_6$ $c_3 = c_2; c_5 = c_6$ $\dot{C}_3 + \dot{C}_5 + \dot{Z}_{eva} = \dot{C}_2 + \dot{C}_6$ $\dot{C}_{eva} = (\dot{c}_3 + \dot{c}_5)\dot{E}x_{ky,eva}$ $f_{c,EVA} = \dfrac{\dot{Z}_{eva}}{\dot{Z}_{eva} + \dot{C}_{eva}}$
Underground circuit 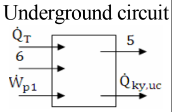	$c_T\dot{E}x_T + c_{w,p1}\dot{W}_{p1} + c_6\dot{E}x_6 + \dot{Z}_{uc} = c_5\dot{E}x_5$ $c_T = 0; c_5 = c_6$ $\dot{C}_{Q,T} + \dot{C}_{w,p1} + \dot{C}_6 + \dot{Z}_{uc} = \dot{C}_5$ $\dot{C}_{uc} = \left(\dot{c}_{Q,T} + \dot{c}_{w,p1} + \dot{c}_5\right)\dot{E}x_{ky,uc}$ $f_{c,UC} = \dfrac{\dot{Z}_{uc}}{\dot{Z}_{uc} + \dot{C}_{uc}}$
Pump 1 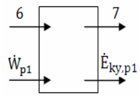	$c_6\dot{E}x_6 + c_{w,p1}\dot{W}_{p1} + \dot{Z}_{p1} = c_7\dot{E}x_7$ $c_5 = c_6 = c_7$ $\dot{C}_6 + \dot{C}_{w,p1} + \dot{Z}_{p1} = \dot{C}_7$ $\dot{C}_{p1} = (\dot{c}_{w,p1} + \dot{c}_6)\dot{E}x_{ky,p1}$ $f_{c,P1} = \dfrac{\dot{Z}_{p1}}{\dot{Z}_{p1} + \dot{C}_{p1}}$
Underground heat exchanger 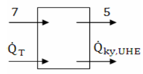	$c_T\dot{E}x_T + c_7\dot{E}x_7 + \dot{Z}_{uhe} = c_5\dot{E}x_5$ $c_5 = c_6 = c_7$ $\dot{C}_{Q,T} + \dot{C}_7 + \dot{Z}_{uhe} = \dot{C}_5$ $\dot{C}_{uhe} = \left(\dot{c}_5 + \dot{c}_{Q,T}\right)\dot{E}x_{ky,uhe}$ $f_{c,UHE} = \dfrac{\dot{Z}_{uhe}}{\dot{Z}_{uhe} + \dot{C}_{uhe}}$
Fan coil circuit 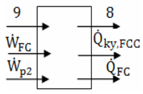	$c_9\dot{E}x_9 + c_{w,p2}\dot{W}_{p2} + c_{w,FC}\dot{W}_{FC} + \dot{Z}_{fcc} = c_8\dot{E}x_8 + c_{FC}\dot{E}x_{FC}$ $c_8 = c_9 = c_{10} = c_{11} = c_{12} = c_{13} = c_{14}$ $\dot{C}_9 + \dot{C}_{w,p2} + \dot{C}_{w,FC} + \dot{Z}_{fcc} = \dot{C}_8 + \dot{C}_{Q,FC}$ $\dot{C}_{fcc} = \left(\dot{c}_9 + \dot{C}_{w,FC} + \dot{c}_{w,p2}\right)\dot{E}x_{ky,fcc}$ $f_{c,FCC} = \dfrac{\dot{Z}_{fcc}}{\dot{Z}_{fcc} + \dot{C}_{fcc}}$
Accumulation tank 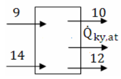	$c_9\dot{E}x_9 + c_{14}\dot{E}x_{14} + \dot{Z}_{at} = c_{10}\dot{E}x_{10} + c_{12}\dot{E}x_{12}$ $c_8 = c_9 = c_{10} = c_{11} = c_{12} = c_{13} = c_{14}$ $\dot{C}_9 + \dot{C}_{14} + \dot{Z}_{at} = \dot{C}_{10} + \dot{C}_{12}$ $\dot{C}_{at} = \dot{c}_9\dot{E}x_{ky,at}$ $f_{c,AT} = \dfrac{\dot{Z}_{at}}{\dot{Z}_{at} + \dot{C}_{at}}$
Pump 2 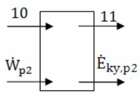	$c_{10}\dot{E}x_{10} + c_{w,p2}\dot{W}_{p2} + \dot{Z}_{p2} = c_{11}\dot{E}x_{11}$ $c_8 = c_9 = c_{10} = c_{11} = c_{12} = c_{13} = c_{14}$ $\dot{C}_{10} + \dot{C}_{w,p2} + \dot{Z}_{p2} = \dot{C}_{11}$ $\dot{C}_{p2} = \left(\dot{c}_{10} + \dot{c}_{w,p2}\right)\dot{E}x_{ky,p2}$ $f_{c,P2} = \dfrac{\dot{Z}_{p2}}{\dot{Z}_{p2} + \dot{C}_{p2}}$
Fan coils 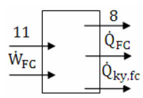	$c_{11}\dot{E}x_{11} + c_{w,FC}\dot{W}_{FC} + \dot{Z}_{FC} = c_8\dot{E}x_8 + c_{FC}\dot{E}x_{FC}$ $c_8 = c_9 = c_{10} = c_{11} = c_{12} = c_{13} = c_{14}$ $\dot{C}_{11} + \dot{C}_{w,FC} + \dot{Z}_{FC} = \dot{C}_8 + \dot{C}_{Q,FC}$ $\dot{C}_{FC} = \left(\dot{c}_{11} + \dot{c}_{w,FC} + \dot{c}_{FC}\right)\dot{E}x_{ky,FC}$ $f_{c,FC} = \dfrac{\dot{Z}_{FC}}{\dot{Z}_{FC} + \dot{C}_{FC}}$
Solar energy circuit 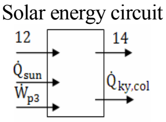	$c_{12}\dot{E}x_{12} + c_{w,p3}\dot{W}_{p3} + \dot{Z}_{sec} = c_{14}\dot{E}x_{14}$ $c_8 = c_9 = c_{10} = c_{11} = c_{12} = c_{13} = c_{14}$ $\dot{C}_{12} + \dot{C}_{w,p3} + \dot{C}_{Q,sun} + \dot{Z}_{sec} = \dot{C}_{14}$ $\dot{C}_{sec} = \left(\dot{c}_{12} + \dot{c}_{w,p3} + \dot{C}_{Q,sun}\right)\dot{E}x_{ky,sec}$ $f_{c,SEC} = \dfrac{\dot{Z}_{sec}}{\dot{Z}_{sec} + \dot{C}_{sec}}$

Table 3. (Continued).

Unit	Exergoeconomic balances
Pump 3 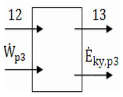	$c_{12}\dot{E}x_{12} + c_{w,p3}\dot{W}_{p3} + \dot{Z}_{p3} = c_{13}\dot{E}x_{13}$ $c_8 = c_9 = c_{10} = c_{11} = c_{12} = c_{13} = c_{14}$ $\dot{C}_{12} + \dot{C}_{w,p3} + \dot{Z}_{p3} = \dot{C}_{13}$ $\dot{C}_{p3} = \left(\dot{c}_{12} + \dot{c}_{w,p3}\right)\dot{E}x_{ky,p3}$ $f_{c,P3} = \frac{\dot{Z}_{p3}}{\dot{Z}_{p3} + \dot{C}_{p3}}$
Solar collectors 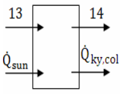	$c_{13}\dot{E}x_{13} + c_{sun}\dot{E}x_{sun} + \dot{Z}_{col} = c_{14}\dot{E}x_{14}$ $c_8 = \ldots = c_{14}; c_{sun} = 0$ $\dot{C}_{13} + \dot{C}_{Q,sun} + \dot{Z}_{col} = \dot{C}_{14}$ $\dot{C}_{col} = \left(\dot{c}_{13} + \dot{C}_{Q,sun}\right)\dot{E}x_{ky,col}$ $f_{c,COL} = \frac{\dot{Z}_{col}}{\dot{Z}_{col} + \dot{C}_{col}}$

relevant costs (the initial investment, maintenance and operating costs), in the second category there are costs from exergy loss and exergy degradation. Evaluations of a component performance are provided by the exergoeconomic factor specific to each component. The exergoeconomic factor for the component of the system is expressed by the following equation [21].

$$f = \frac{\dot{Z}}{\dot{Z} + c\dot{E}x_{ky}} . \tag{25}$$

The exergoeconomic balance of the overall system is shown in Eq. (26) below:

$$\dot{C}_{Q,T} + \dot{C}_{W,comp} + \dot{C}_{W,p1} + \dot{C}_{W,p2} + \dot{C}_{W,p3} + \dot{C}_{W,FC} + \dot{C}_{Q,sun} + \dot{Z}_{sys} = \dot{C}_{Q,FC} . \tag{26}$$

The exergoeconomical value from the structure and operation of the system is calculated as an economic value Eq. (27):

$$\dot{Z}_{sys} = \dot{Z}_{sys}^{production} + \dot{Z}_{sys}^{operating} + \dot{Z}_{sys}^{waste} . \tag{27}$$

Exergoeconomic factor is calculated by Eq. (28) below:

$$f_{sys} = \frac{\dot{Z}_{sys}}{\dot{Z}_{sys} + \dot{C}_{sys}} . \tag{28}$$

With the help of the defined exergoeconomic equations, the exergoeconomic equations and exergoeconomic factors for overall systems and units are given in Table 3.

4. Results and discussions

The experimental studies have been divided into 3 main parts. The first part covers an energy analysis, the second part covers an exergy analysis and the investigation of its yield, and the third part covers the exergoeconomic analysis and calculation of the exergoeconomic factor. The system properties consist of 4 circuits and 11 units in the heating process. Analyses were performed separately for the system's chosen control volumes.

Table 4. The values detected for nodal points in the heating process.

Node No.	Stage	$\dot{m}$ [kg/s]	T [°C]	h [kj/kg]	s [kj/kgK]
1	Gas	0.09566	65.0	456.58	1.827
2	Liquid	0.09566	8.8	418.70	1.788
3	Wet steam	0.09566	3.1	263.14	1.220
4	Gas	0.09566	41.8	263.14	1.211
5	Liquid	0.900	9.3	39.060	0.141
6	Liquid	0.900	4.7	19.757	0.072
7	Liquid	0.900	4.6	19.337	0.070
8	Liquid	0.575	35.1	146.982	0.506
9	Liquid	0.575	42.8	179.165	0.610
10	Liquid	0.575	42.6	178.322	0.607
11	Liquid	0.575	42.5	177.900	0.605
12	Liquid	0.100	37.4	156.601	0.538
13	Liquid	0.100	37.3	156.180	0.536
14	Liquid	0.100	41.5	173.720	0.592

Table 5. The values obtained for nodal points in the heating process.

Node No.	Stage	$\dot{E}$ [kW]	$\dot{E}x$ [kW]
1	Gas	43.676	6.8496
2	Liquid	40.053	4.2451
3	Wet steam	25.172	4.2058
4	Gas	25.172	4.4409
5	Liquid	35.154	0.5272
6	Liquid	17.781	0.1172
7	Liquid	17.403	0.2309
8	Liquid	84.515	5.0647
9	Liquid	103.020	7.2355
10	Liquid	102.535	7.2220
11	Liquid	102.293	7.2934
12	Liquid	15.660	0.9686
13	Liquid	15.618	0.9812
14	Liquid	17.372	1.2055

* $\dot{W}_{comp} = 4.530$ kW, $\dot{W}_{p1} = 0.176$ kW, $\dot{W}_{p2} = 0.090$ kW, $\dot{W}_{p3} = 0.040$ kW, $\dot{W}_{FC} = 0.300$ kW, $\dot{Q}_{sun} = 2.464$ kW, $\dot{E}x_{sun} = 2.348$ kW, $\dot{Q}_T = 17.751$ kW, $\dot{E}x_T = 0.8183$ kW, $\dot{Q}_{FC} = 16.3558$ kW, $\dot{E}x_{FC} = 2.035$ kW

4.1 Energy analysis evaluation of the system

In this study, the variable parameters were the temperature, pressure and flow values. In Table 4, there are the measured values of the system's nodes. In Table 5, there are energy and exergy values in units of time which were calculated in accor-

Table 6. The average heat values of the components in the heating process.

SYSTEM	$\dot{E}_{in}$ [kW]	$\dot{E}_{out}$ [kW]	$\dot{E}_{ky}$ [kW]	η_I [%]
ALL SYS	25.351	16.3558	8.9952	64.52
COND	128.192	128.192	0.000	100.00
COMP	44.583	43.676	0.907	79.98
EVA	60.326	57.834	2.492	85.66
TV	25.172	25.172	0.000	100.00
P1	17.957	17.403	0.554	46.56
UHE	35.154	35.154	0.000	100.00
AT	120.392	118.195	2.197	28.33
FC	102.593	100.871	1.722	90.47
P2	102.625	102.293	0.332	37.19
COL	18.082	17.372	0.710	71.19
P3	15.700	15.618	0.082	95.23

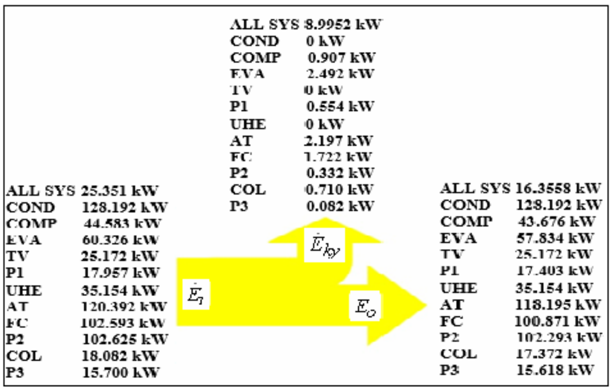

Fig. 4. A Sankey diagram of the system's average energy loss.

dance with the equations in part 3 in terms of the averages of the flow and temperature values measured in the heating process, Solkane and Coolpack programs for the R407C refrigerant fluid, thermodynamic tables for water, and enthalpy and entropy values which were obtained from the EES program.

For the heating process, an energy analysis was performed according to the ratio of the system's input and output energy amounts in units with boundaries which were determined by the equations used in Table 2, and using the values given in Tables 4 and 5. The energy analysis' results are given in Table 6. Monthly average temperatures and meteorological values which were obtained during the heating process was given in Table 7.

In Table 6, the energy efficiency is calculated by the amount of input, output and energy loss of each system component. In Fig. 4, the average energy loss of system and each component was given in a Sankey diagram. According to these results;

- Since the underground heat exchanger, the condenser and the throttle valve were considered to have less dissipation, their heat loss was not seen. The evaporator and condenser are steel plate heat exchangers, and it was determined that the evaporator's energy loss amount was 2.492 kW, and it worked at an 85.66 % energy efficiency.
- The compressor is a scroll type, and it was determined that the energy loss amount was 0.907 kW, and the energy efficiency level was at 79.98 %. During the time of these measurements, the average power consumed by the compressor was 4.530 kW and the total average power consumed by the system was 5.136 kW.
- The accumulation tank transferred heat with an efficiency of 28.33 %, and the aim of this tank is to always keep the water at the required temperature for the fan coils only.
- The pump's energy loss amount was very low in the system. In the fan coil, energy loss amount was 1.722 kW and there was 90.47 % energy efficiency. The average power consumed by the fan coil was measured to be at 0.300 kW.
- The collector's energy loss amount was determined to be 0.710 kW, and the energy efficiency was found to be at 71.19 %.

Table 7. The monthly average temperatures and meteorological values obtained during the heating process.

	Q_T [kW]	T_{100m} (°C)	T_{ex} (°C)	COP_H (SYS)	COP_H (HP)
November	18.079	14.1	11.2	3.62	4.07
December	17.617	13.5	5.2	3.60	4.06
January	17.927	13.8	6.1	3.61	4.09
February	17.887	13.2	4.8	3.60	4.06
March	17.790	14.2	11.8	3.65	4.12

In Table 7, the exterior temperature in the heating process (November 1st, 2013 – March 31st, 2014) was measured to be at an average of 4.8 °C in February, the coldest month, and at an average of 11.8 °C in March, the warmest month. The overall average for the noted heating period was 8.0 °C. The ground's temperature at the depth of 100 meters into the well was measured to be at an average of 13.2 °C in February, at an average of 14.2 °C in March, and at an overall average 13.8 °C. For this reason, it was seen that the heat interchange taken from the ground by the system varied between 17.617-18.079 kW in proportion to the exterior temperatures as the result of the measurements and calculations. In order to compensate for the heat loss of the room in the investigation process, water was to be prepared at the temperature of 42.3-43.1 °C in the accumulation tank depending on the measured exterior temperature. In this process, the power consumed by the compressor, three circulation pumps and the fan coil was measured to be at an average of 5.136 kW. The heat transferred by the system to the test room was affected relatively more by the interchange in exterior temperature, and this value changed between 16.102-16.411 kW. The system's_energy analysis results were compared with those in the Refs. [22, 23] and it was determined that the COP values were relatively better, and also occurred at the determined intervals. It has

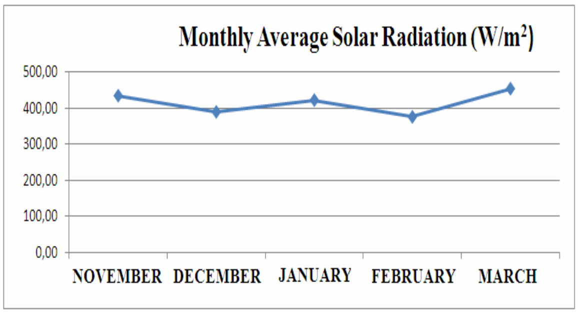

Fig. 5. The monthly average solar radiation value in the heating process.

been determined that the system provides the required amount of energy from the soil and that the system fully meets the heating requirement of the test area.

The heating seasons' monthly average solar radiation value was given in Fig. 5. The solar energy system provided hot water for the accumulation tank to sustain the system during the heating season. The hot water support provided to the accumulation tank by the solar energy system was saved the operating time of the compressor. With the two collectors used in this context, the highest amount of energy was obtained as 1.785 kW in March when sunshine is maximal, and at 1.454 kW in February, when sunshine is minimal. The obtained energy amount was transferred from the collectors to the accumulation tank via fluid. When Eq. (14) is used to investigate the assistance obtained from the solar energy in relation to climate changes, the solar energy coverage ratio was calculated to be at an average of 10.34 % in November, an average of 9.48 % in December, an average of 9.66 % in January, and average of 10.43 % in March. Depending on the number of solar collectors, the support provided to the system was in the ranges specified in the Ref. [24].

4.2 Exergy analysis evaluation of the system

By benefiting from the equations given in Table 2 and the values given in Table 4 - which were specially prepared for the system's components - the input exergy amount, output exergy amount, exergy loss amount and second law's efficiency towards each system component were calculated, and these values are given in Table 8. The Sankey diagram of the system's average exergy loss and each component in it was given in Fig. 6.

By examining Table 8 and Fig. 6, the highest exergy loss observed in the compressor with 1.9255 kW, on the other hand, the lowest exergy destruction determined in the throttling valve, condenser and accumulation tank as 0.2351 kW, 0.2379 kW and 0.2504 kW, respectively. This system evaluation in terms of exergy efficiency, the highest exergy efficiency obtained condenser with 98 % and accumulation tank with 97.03 %, conversely, the lowest exergy efficiency determined in the solar collectors with 36.21 %. In addition, exergy efficiency of all system calculated as 24.51 %.

Table 8. The average exergy values of components in the heating process.

SYSTEM	$\dot{E}x_i$ [kW]	$\dot{E}x_o$ [kW]	$\dot{E}x_{ky}$ [kW]	η_{II}[%]
ALL SYS	8.3023	2.035	6.2673	24.51
COND	11.9143	11.6764	0.2379	98.00
COMP	8.7751	6.8496	1.9255	78.06
EVSA	4.7330	4.3623	0.3707	92.17
TV	4.4409	4.2058	0.2351	94.71
UHE	1.0492	0.5272	0.5220	50.25
AT	8.4410	8.1906	0.2504	97.03
FC	7.5934	7.0997	0.4937	93.50
COL	3.3292	1.2055	2.1237	36.21

Table 9. The distribution of the monthly average exergy loss.

SYSTEM	$\dot{E}x_{ky}$ [kW] NOV	$\dot{E}x_{ky}$ [kW] DEC	$\dot{E}x_{ky}$ [kW] JAN	$\dot{E}x_{ky}$ [kW] FEB	$\dot{E}x_{ky}$ [kW] MAR
ALL SYS	6.2134	6.4016	6.2767	6.1181	6.1810
CON	0.1258	0.1190	0.3078	0.3206	0.1039
COMP	1.9418	1.9543	1.9114	1.9242	1.8606
EVA	0.3343	0.4171	0.3975	0.4045	0.3335
TV	0.2214	0.2351	0.2481	0.2467	0.2346
UHE	0.5552	0.5399	0.4476	0.4331	0.5516
AT	0.2049	0.3136	0.3025	0.2965	0.2729
FC	0.4700	0.4756	0.4872	0.4968	0.4841
COL	2.2566	2.2344	2.0603	1.8807	2.2303

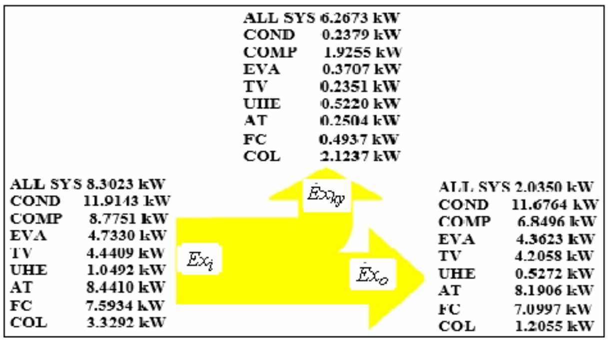

Fig. 6. A Sankey diagram of the exergy loss averages.

In Table 9, the heating process's monthly average exergy loss distribution is given. The highest exergy loss values occurred in the month of the December. In that month, compressor had the highest exergy loss value. As a result of compressor switches, this situation occurred frequently. By examining this table, the system's elements can be compared with each other. At the same time, the effects of climate changes can be observed. This value changes against the outdoor air temperature and with the evaporator, condenser, accumulation tank and the collectors. According to the assumptions and calculations, this value does not depend on the outdoor air tempera-

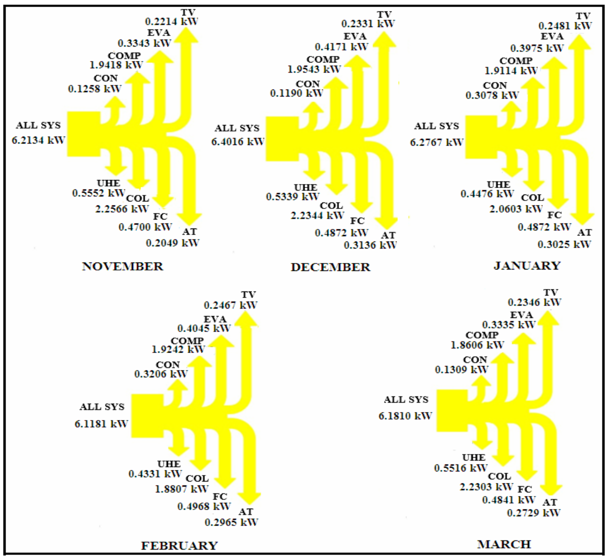

Fig. 7. A Sankey diagram of the monthly average exergy losses.

ture for the throttling valve. Furthermore, the Sankey diagram of the system's monthly average exergy loss of elements during the heating process was given in Fig. 7. The sun collectors and compressor have been identified as the components with the most serious exergy losses in the system. They were followed by UHE and FC.

4.3 Exergoeconomic analysis evaluation of the system

By using the equations which have been designed for the system's elements and given in Table 3, the exergoeconomic analysis results during the heating process are shown in Table 10. The results of the exergoeconomic analysis are shown in Figs. 8-10. In this study, three main values that were used as economic parameters. These are the levelized total cost, exergy cost and exergoeconomic factors. For the whole system, these values were calculated to be at the levelized total cost of \$1.2268/h, exergy cost of \$0.8005/h, and exergoeconomic factor of 60.51 %. In Fig. 8, the changes to the levelized total cost depending on the system's elements during the heating process are shown. According to the assumptions and calculations, the compressor had the highest value at \$0.4658/h. The values of the other elements are shown in Table 10. As seen in Table 10 and Fig. 8, the levelized total cost was not affected by outdoor air temperature change. This value was the highest in the compressor at \$0.4658/h and in the underground heat exchanger at \$0.1587/h.

In Fig. 9, the monthly average exergy cost distributions for the system elements during the heating process are shown. By examining Fig. 9, the system elements can be compared, and the effects of climate changes can be observed. The averages change depending on the interchange in the exterior temperature. For other components, the air temperatures' interchanges can be seen in a relatively reverse direction at the collectors, fan coil, and throttle valve, as well as other components. The component with the highest exergy cost was the compressor.

The system components' monthly average exergoeconomic factor values in the heating process are given in Fig. 10. By investigating Fig. 10, the effects of climate change can be seen

Table 10. The average exergoeconomic analysis results.

SYSTEM	$\dot{Z}$ [\$/h]	$\dot{C}$ [\$/h]	f [%]
ALL SYS	1.2268	0.8005	60.51
COND	0.1208	0.1234	49.47
COMP	0.4658	0.7108	39.59
EVA	0.1208	0.2095	36.57
TV	0.0107	0.0703	13.20
UHE	0.1587	0.1389	53.33
AT	0.0276	0.0550	33.41
FC	0.1553	0.1888	32.32
COL	0.0966	0.4861	16.58

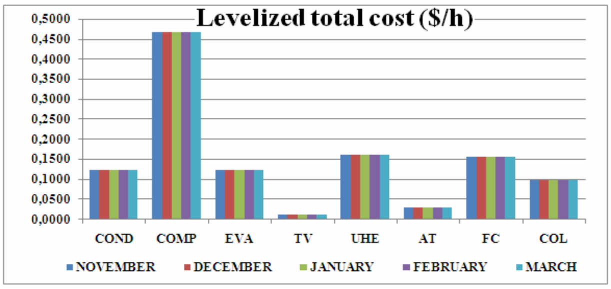

Fig. 8. The variations between levelized total costs.

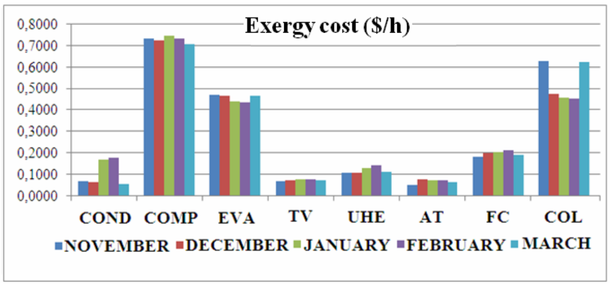

Fig. 9. The variations between exergy costs.

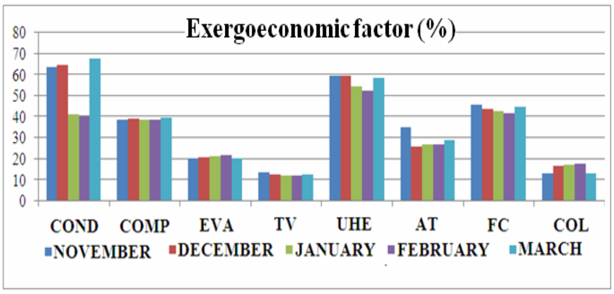

Fig. 10. The variations between exergoeconomic factors.

Table 11. Cost comparison of the systems.

System and components	Power consumption	$\dot{C}$ [\$/h]	$\dot{Z}$ [\$/h]
SE assisted VGSHP+ FC (VSGHP, 2COL, AT, 2FC, 3Pumps)	2720 kWh_e	0.282	1.227
ASHP+FC (HKIP,2 FC, AT, 2Pumps)	3445 kWh_e	0.347	1.436
Chiller+ FC (Chiller, AT, 2FC, 2Pumps)	5252 kWh_e	1.072	1.370
Split air conditioner sys. (internal and external units)	3652 kWh_e	1.066	1.358
Combi boiler+ FC (Combi boiler, AT, 2FC, 2Pumps)	460 kWh_e 1286 Nm^3 NG	0.976	1.448

while comparing the system components with each other. The exergoeconomic value changes depend on the exterior temperatures. The exergoeconomic factor value is directly related to a levelized total cost value. The exergoeconomic factor was small for each system element, which reduced the exergy destruction, so savings can be made. However, for larger exergoeconomic factors, the elements' initial investment cost was larger in comparison to the exergy efficiencies. In this case, efforts to reduce the initial investment costs should be a priority. The typical values of the exergoeconomic factors varied to suit the correlating element in the literature. For example, these values were typically 55 % for the heat exchangers, between 35 % and 75 % for the compressors and turbines and 70 % for pumps [25]. In Table 10 and Fig. 10, the changes in the exergoeconomic factors in the heating process are shown. According to this assessment, there was a 39.59 % at the compressor. For the system components, the exergoeconomic values were less than the 55 % reported in the literature for heat exchangers. In the system, low exergoeconomic factors were observed, so to raise the exergoeconomic factor, the exergy loss and exergy costs should be reduced.

4.4 Solar energy assistance

The heat which is obtained from the two solar collectors used during the heating seasons is intended to sustain the heat pump system by transferring it to the accumulation tank. When that solar energy assistance was investigated as it's used during the heating process, the energy requirement coverage ratio of the system was calculated to be at an average of 9.75 %. As a result, the expected solar energy assistance ratio was provided according to the number of collectors during the heating season. It should also be considered that more assistance can be provided by introducing more collectors.

4.5 Comparison of systems

The power consumption of the solar-assisted VGSHP proposed in this study was compared with four different electricity consuming systems in terms of their levelized cost values, and the system components and costs are given in Table 11.

As a result, the investigated system is the most economical one among the investigated systems in terms of both its energy cost and total cost. Although the initial investment cost of the system is high, it is seen that it is the most economical system among the comparable systems which amortize itself on an average of four years.

5. Conclusion

In this study, it has been seen that the highest energy loss amount among the system components was at the evaporator with 2.492 kW. As a result of the energy analysis, it was seen that the system operation was affected by the exterior temperatures. Accordingly, the COP value of the overall system was determined to be at an average 3.61. Although the COP value of the heat pump device was found to be 4.09, the COP value decreased to 3.61 when investigated together with the fan coil group. The decrease resulted from the loss of distance between the heat pump and fan coil.

According to the results of the system components' exergy and exergoeconomic analyses, the highest exergy losses of the components in the heating process were determined to be at the collectors and compressor. As a result of the exergoeconomic analysis, the highest levelized total cost was found to be at \$0.4658/h for the compressor. It was followed by the UHE at \$0.1587/h. For the collector with the highest exergy loss, this value was calculated to be \$0.0966/h. It has been seen that the system components' variety of exergy costs was also an effect of the exterior temperatures during the heating process. The component with the highest exergy cost was calculated to be the compressor at \$0.7108/h. In terms of the exergy loss ratio (which was obtained by dividing the exergy loss amount of one component by the exergy loss amount of the whole system), the components with the highest value were determined to be the collector, with 33.89 %, and the compressor, with 30.72 %. The exergoeconomic factor values were calculated to be 39.59 % for the compressor and 16.58 % for the collectors. If the exergoeconomic factor calculated for any system component is a small value, it indicates that savings can be made by reducing the exergy loss of the relevant component. On the other hand, if exergoeconomic factor is a large value, it means that the initial investment cost of the component is relatively higher than the exergy efficiency. In this case, it is primarily necessary to carry out studies for reducing the initial investment cost of the relevant components [21]. In this context, the components causing the highest system exergy loss are the collectors and compressors (during the heating seasons). From the perspective of the initial investment costs, the initial investment cost of the collector was very low compared to that of the compressor. Since the collector's exergy loss was directly related to solar radiation, improvements should be considered for the compressor. From the perspective of these improvements, it is primarily possible to make the compressor less engaged. Thus, there will be less electricity consumption, and reduction in its exergy losses. For this, the heat pump's operating temperature range can be increased in the heat pump software, and frequency converter compressors can be selected. The heat pump will thus be able to operate longer in lower temperature regimes, and thus the compressor's efficiency will be higher.

As a result, if the ground heat exchanger's and excavation costs are reduced and the heat pump is produced with domestic technology, the use of these systems for our country will be beneficial both economically and environmentally. Our system is highly effective in reducing both energy consumption and the emissions of greenhouse gases. It seems appropriate to use the system for the province Mardin, which currently takes advantage of fossil fuels to heat itself. Therewithal, it is thought that the use of such systems in regions with similar climate zones will be beneficial for alleviating some economic and environmental strain. In order to make the use of such systems widespread, more studies have to be done and supported by governments.

Nomenclature

A	: Area [m^2]; a levelized value factor
ASHP	: Air source heat pump system
AT	: Accumulation tank
$\dot{C}$	: Exergy cost [$/h]
c	: Unit exergy cost [$/kJ]
CELF	: Constant escalation levelling factor
COMP	: Compressor
COP	: Coefficient of performance
CRF	: Initial investment recovery factor
c_p	: Specific heat [kJ/kg°C]
E	: Energy [kJ]
$\dot{E}$	: Flow of energy [kW]
$\dot{E}_{ky}$	: Energy loss [kW]
$\dot{E}x$	: Flow of exergy [kW]
$\dot{E}x_{ky}$	: Exergy loss [kW]
f	: Exergoeconomic factor
FC	: Fan coil
GSHP	: Ground source heat pump
h	: Enthalpy [kJ/kg]
H	: Heating; higher value
$\overrightarrow{Ht}$	: Total amount of energy from solar radiation [kW]
HGSHP	: Horizontal ground source heat pump
HP	: Heat pump
HPC	: Heat pump circuit
i	: Effective interest rate [%]
i_{eff}	: Repayment ratio
k	: Levelized price correction factor
KH	: Control volume
ky	: Loss
L	: Lower value
$\dot{m}$	: Mass flow [kg/s]
η	: Efficiency [%]
NG	: Natural gas
Q	: Heat energy [kJ]
$\dot{Q}$	: Heat flux [kW]
P	: Pump
$P1$	: Pump1
$P2$	: Pump2
$P3$	: Pump3
R	: Heat resistance [W/m^2. K], correction factor for SE
r_i	: Stated rate of interest [%]
r_n	: Nominal escalation value [%]
s	: Entropy for unit mass [kj/kgK]; inclination angle
SE	: Solar energy
SEC	: Solar energy circuit
th	: Thermic
T	: Temperature [°C, K]
TV	: Throttling valve
u	: Internal energy for unit mass [kj/kg]
UC	: Underground circuit
UHE	: Underground heat exchanger
VGSHP	: Vertical ground source heat pump
W	: Work [kj]
$\dot{W}$	: Power [kW]
$\dot{Z}$	: Levelized total cost [$/h]

Subscripts

at	: Accumulation tank
col	: Solar collector
cond	: Condenser
comp	: Compressor
e	: Electricity; equivalent
eva	: Evaporator
ex	: Exterior
fc	: Fan coil
fcc	: Fan coil circuit
h, H	: Heating
hp	: Heat pump
hpc	: Heat pump circuit
i	: Input
in	: Input
k	: Each system part
ky	: Loss
n	: Specified lifetime of systems or components (year)
o	: Output
out	: Output
0	: Reference state
p	: Pump
q	: Heat
sec	: Solar energy circuit
sys	: System
sun	: Sun
T	: Ground, soil
tv	: Throttling valve
uc	: Underground circuit
uhe	: Underground heat exchanger
w	: Work

References

[1] *Energy analysis*, TC Anadolu University Publication, No: 2486, 1. Edition, May, Eskişehir, Turkey (2012).

[2] U. Akbulut, Theoretical and experimental investigation of a renewable energy source assisted heating and cooling system, *Doctora Thesis*, Yıldız Technical University FBE, İstanbul, Turkey (2012).

[3] T. B. Yüksel, Investigation of biogas, solar and ground energy assisted greenhouse heating, *Doctora Thesis*, Fırat Universty FBE, Elazığ, Turkey (2011).

[4] J. G. Cervantes and E. Torres-Reyes, Experiments on a solar assisted heat pump and an exergy analysis of the system, *Applied Thermal Engineering*, 22 (2002) 1289-1297.

[5] Y. Bi, T. Guo, L. Zhang and L. Chan, Solar and ground source heat pump system, *Applied Energy*, 78 (2004) 231-245.

[6] O. Özgener and A. Hepbaşlı, Exergoeconomic analysis of a solar assisted ground-source heat pump greenhouse heating system, *App. Thermal Eng.*, 25 (2005) 1459-1471.

[7] Ö. Özgener and A. Hepbaşlı, A review on the energy and exergy analysis of solar assisted heat pump systems: An experimental study, *Renewable and Sustainable Energy Reviews*, 11 (2007) 482-496.

[8] Ö. Özgener, A. Hepbaşlı and L. Özgener, A parametic study on the exergoeconomic assessment of a vertical ground-coupled(geothermal) heat pump system, *Building and Environment*, 42 (2007) 1503-1509.

[9] G. Tsatsaronis, Definitions and nomenclature in exergy analysis and exergoeconomics, *Energy*, 32 (2007) 249-253.

[10] H. Esen, M. İnallı, M. Esen and K. Pıhtılı, Energy and exergy analysis of a ground-coupled heat pump system with two horizontal ground heat exchangers, *Building and Environment*, 42 (2007) 3606-3615.

[11] A. Dikici and A. Akbulut, Performance characteristics and energy and exergy analysis of solar assisted heat pump, *Building and Environment*, 43 (2008) 1961-1972.

[12] Y. Bi, X. Wang, Y. Liu, H. Zhang and L. Chen, Comprehensive exergy analysis of a ground source heat pump system for both building heat and cooling modes, *Applied Energy*, 86 (2009) 2560-2565.

[13] K. Bakırcı, Ö. Özyurt, K. Çomaklı and Ö. Çomaklı, Energy analysis of a solar-ground source heat pump system with vertical closed-loop for heating applications, *Energy*, 36 (2011) 3224-3232.

[14] E. Kim, J. Lee, Y. Jeong, Y. Hwang¸ S. Lee and N. Park, Performance evaluation under the actual operating condition of a vertical heat pump system in a school building, *Energy and Buildings*, 50 (2012) 1-6.

[15] Ş. M. Acar and O. Arslan, Exergo-economic evaluation of a new drying system boosted by ranque-hilsch vortex tube, *Applied Thermal Engineering*, 124 (2017) 1-16.

[16] E. Akrami, A. Chitsaz, P. Ghamari and S. M. S. Mahmoudi, Energy and exergy evaluation of a tri-generation system driven by the geothermal energy, *Journal of Mechanical Science and Technology*, 31 (1) (2017) 401-408.

[17] İ. Ceylan, H. Doğan and K. Yalçın, Experimental comporasion of prismatic type solar collector as energy productivity, *Teknoloji*, 7 (3) (2004) 395-400.

[18] J. A. Duffie and W. A. Beckman, *Solar engineering of thermal process*, A Wiley-İnterscience Publication, Second Edition, John Wiley & Sons İnc. (1991).

[19] M. A. Rosen, Exergy conservation; An alternative to conserving the already conserved quantity energy, *Exergy an İnternational Journal*, 2 (2002) 59-61.

[20] G. Temir and D. Bilge, Thermodynamic analysis of a trigeneration system, *Applied Thermal Eng.*, 25 (2004) 411-422.

[21] A. Bejan, G. Tsatsaronis and M. Moran, *Thermal design and optimization*, John Wiley and Sons Inc., USA (1996).

[22] O. Ozyurt and D. A. Ekinci, Experimental study of vertical ground-source heat pump performance evaluation for cold climate in Turkey, *Applied Energy*, 88 (2011) 1257-1265.

[23] J. Luo, J. Rohn, M. Bayer, A. Priess, L. Wilkmann and W. Xiang, Heating and cooling performance analysis of a ground source heat pump system in Southern Germany, *Geothermics,* 53 (2015) 57-66.

[24] X. Chen, Y. Hongxing, L. Lin, W. Jinggang and L. Wei, Experimental studies on a ground coupled heat pump with solar thermal collectors for space heating, *Energy,* 36 (2011) 5292-5300.

[25] U. Akbulut, Z. Utlu and O. Kincay, Exergy, Exergoenvironmental and exergoeconomic evaluation of a heat pump-integrated wall heating system, *Energy*, 107 (2016) 502-522.

Fatih Ünal graduated from mechanical engineering in Dumlupınar University with a high degree of honor in 2006. Fatih Ünal graduated his master and Ph.D. in Yıldız Technical University in 2009 and 2014, respectively. He has been working as an academician at Mardin Artuklu University since 2009. He is currently the Head of the Department of Machinery and Metal Technologies Program. He studies in the fields of energy, exergy, renewable energy and heat transfer.